*J. Astrophys. Astr.* (2021)42:1
https://doi.org/10.1007/s12036-020-09653-8



# Turbulence generation of ion scale in the presence of magnetic islands and guide field at the magnetopause region

RAJESH KUMAR RAI[1], NEHA PATHAK[2,*], PRACHI SHARMA[3], SWATI SHARMA[4], NITIN YADAV[5] and R. P. SHARMA[2]

[1]Department of Physics, D.A.V.P.G. College, Gorakhpur 273 001, India.
[2]Centre for Energy Studies, Indian Institute of Technology Delhi, Delhi 110 016, India.
[3]Madhav Institute of Technology and Science, Gwalior 474 005, India.
[4]Department of Physics, University of Rajasthan, Jaipur 302 004, India.
[5]Max-Planck-Institut fur Sonnensystemforschung, Gottingen, Germany.
*Corresponding Author. E-mail: npsneha90@gmail.com

MS received 29 July 2019; accepted 28 September 2020

**Abstract.** In the present work, turbulence generation due to the dynamic evolution of magnetic islands is investigated. The role of ambient magnetic field in the evolution of magnetic islands and turbulence generation is also investigated. The origin of magnetic islands lies in the fact that reconnection takes place in thin current sheets which becomes unstable and leads to the formation of magnetic islands. The model is developed using basic fluid equations and Maxwell's equations to study the dynamics of magnetic islands. The dynamical equation has been solved numerically for two different cases: (a) background field consisting of Harris equilibrium field component only and (b) background field comprising of both axial and Harris equilibrium field. It is evident from our investigation that the evolution of magnetic islands establishes the presence of turbulence in reconnection sites. Using the simulation data, we have also examined the associated power spectrum which displays the distribution of energy in different wave modes. This spectral index has consistency with THEMIS observations (Chaston *et al*. 2008, *Nat. Phys*. 4, 19). In this way, the present approach may be helpful to understand the interplay between magnetic reconnection and turbulence in magnetopause region.

**Keywords.** Magnetic reconnection—magnetic islands—turbulence.

## 1. Introduction

Turbulence is a natural state of space plasmas and described as an admixture of random fluctuations on many different scales. It is an energy transfer process in a medium by which energy is injected at large scales and converted into motions at smaller scales. In general, magnetic field lines play an important role in many astrophysical and space plasmas, to develop theoretical explanations of dynamical processes such as magnetic reconnection (Parker 1979). The reconfiguration in magnetic field lines and resulting rapid transfer of energy from fields to particles, has been observed by Magnetospheric Multiscale misson (MMS) in the Earth's magnetosphere (Burch *et al*. 2016; Eastwood *et al*. 2009). The breaking and reforming of magnetic fields are broadly used in describing mechanisms for particle acceleration and transport of energetic particles.

When oppositely directed magnetic field lines approach each other and reconnect in a current sheet, where magnetic X-line configuration is formed, the magnetic island is formed between two X-lines (Parker 1957; Sweet 1958). Thus the reconfiguration of magnetic field lines leads to the generation of magnetic islands (Wang *et al*. 2010; Daughton *et al*. 2011; Dong *et al*. 2012). It plays a key role in electron acceleration in reconnection sites. In literature, various mechanisms have been suggested to explain the electron acceleration during the evolution of magnetic

Published online: 04 February 2021

reconnection such as the contributions of the parallel electric field, Fermi and betatron mechanisms. One of the important mechanism is the interaction between magnetic islands (Ambrosiano *et al*. 1988). Chen *et al*. (2008) have suggested the link between energetic electrons and magnetic islands during reconnection in the Earth's magnetosphere. Magnetic islands can support in enhancing the reconnection rate and the efficiency of particle acceleration (Daughton *et al*. 2006; Bhattacharjee *et al*. 2009; Matthaeus & Lamkin 1985; Fu *et al*. 2006; Chen *et al*. 2008; Takasao *et al*. 2016).

In the present work, we have developed a model using EMHD model, to examine the effect of guide field and thickness of Harris sheet on the evolution of magnetic islands and turbulence generation. The model equation is solved numerically for magnetopause region parameters using pseudo spectral method and finite difference method.

In the present work, we are investigating the role of the background magnetic field in the evolution of magnetic islands. The model equations for island evolution have been obtained using two-fluid model and solved numerically for magnetopause region parameters.

The contents of the paper are organized as follows: Section 2 presents the dynamics of basic equations. Numerical simulation results have been discussed in Section 3. The paper concludes with Section 4 by providing the summary and discussion.

## 2. Basic formulations

The model equations are developed in 3D using two-fluid equations and Maxwell's equations and their evolution in time has been studied. In this analysis, we have assumed that background magnetic field $\vec{B}$is along $z$ direction.

One can obtain model equations in the following steps: electron momentum equation is written as

$$\frac{\partial \vec{v}_e}{\partial t} = -\frac{e}{m_e}\vec{E} - \frac{e}{cm_e}\left(\vec{v}_e \times \vec{B}\right) - \frac{k_B T_e}{n_0 m_e}\vec{\nabla} n. \tag{1}$$

Here, $n_0$ is the background density, $n$ is the density perturbation in the background density, $T_e$ is the electron temperature, $k_B$ is the Boltzmann constant and $\vec{v}_e$ is electron velocity. Taking parallel component of electron equation of motion and using $E_z = -\nabla_z \phi - \frac{1}{c}\frac{\partial \tilde{\psi}}{\partial t}\hat{z}$,

$$\frac{1}{c}\frac{\partial \tilde{\psi}}{\partial t} + \frac{\vec{B}\cdot\vec{\nabla}\phi}{B} + \frac{k_B T_e}{n_0 e}\vec{\nabla}_z n + \frac{m_e}{n_0 e}\frac{\partial j_{ez}}{\partial t} = 0. \tag{2}$$

Here, $\vec{j}_{ez} = -n_0 e \vec{v}_{ez}$ is the current density. Equation (2) can be re-written as

$$\frac{\partial \tilde{\psi}}{\partial t} + \frac{c}{B}\vec{B}\cdot\vec{\nabla}\phi + \frac{c k_B T_e}{n_0 e}\vec{\nabla}_z n + \frac{c m_e}{n_0 e}\frac{\partial j_{ez}}{\partial t} = 0. \tag{3}$$

Using the Ampere's law, the current density ($j_{ez}$) can be written as

$$j_{ez} = -\frac{c}{4\pi}\nabla_\perp^2 \tilde{\psi}. \tag{4}$$

Using quasi neutrality condition $\vec{\nabla}\cdot\vec{j} = 0$ (here $\vec{j} = -n_0 e(\vec{v}_e - \vec{v}_i)$ is the current density, $v_e$ and $v_i$ are the electron and ion velocities respectively), we get

$$\vec{\nabla}_\perp \cdot \vec{v}_{i\perp} + \frac{1}{n_0 e}\nabla_z \cdot j_{ez} = 0. \tag{5}$$

The perpendicular component of ion velocity can be given as

$$\vec{v}_{i\perp} = \left(\frac{c}{B}\right)\vec{E}_\perp \times \hat{z} + \left(\frac{c}{\omega_{ci}B}\right)\frac{\mathrm{d}}{\mathrm{d}t}\vec{E}_\perp. \tag{6}$$

Here, $\omega_{ci} = eB/m_i c$ is the ion gyrofrequency. Taking the divergence of the above equation, it can be written as

$$\vec{\nabla}_\perp \cdot \vec{v}_{i\perp} = -\frac{c}{\omega_{ci}B}\frac{\mathrm{d}}{\mathrm{d}t}\left(\nabla_\perp^2 \phi\right). \tag{7}$$

By using the relation $\frac{d}{dt} = \frac{\partial}{\partial t} + v\cdot\nabla$ in Equation (7), it can be written as

$$\vec{\nabla}_\perp \cdot \vec{v}_{i\perp} = -\frac{c}{\omega_{ci}B}\left(\frac{\partial}{\partial t} + \vec{v}\cdot\vec{\nabla}\right)\left(\nabla_\perp^2 \phi\right). \tag{8}$$

Using Equation (8) in Equation (5), it can be written as

$$\left(\frac{\partial}{\partial t} + v\cdot\nabla\right)\nabla_\perp^2 \phi = \frac{B\omega_{ci}}{cn_0 e}\nabla_z \cdot j_{ez}. \tag{9}$$

From electron continuity equation, we get

$$\left(\frac{\partial}{\partial t} + \vec{v}\cdot\vec{\nabla}\right)n = \frac{1}{e}\nabla_z j_{ez}. \tag{10}$$

The density modification is written in terms of scalar potential with the help of Equations (9) and (10) as

$$n = \frac{n_0 c}{B\omega_{ci}}\nabla_\perp^2 \phi. \tag{11}$$

Equation (3) can be written by using Equation (4) in (11) as

$$\frac{\partial\tilde{\psi}}{\partial t}+\frac{c}{B}\vec{B}\cdot\vec{\nabla}\phi-\frac{c^2k_BT_e\nabla_\perp^2}{e\omega_{ci}B}\vec{B}\cdot\vec{\nabla}\phi-\frac{c^2m_e\nabla_\perp^2}{4\pi n_0e}\frac{\partial\tilde{\psi}}{\partial t}=0. \quad (12)$$

By using a small field perturbation $\vec{b}$ (where $\vec{b}=\vec{\nabla}\times\tilde{\psi}$) in the background magnetic field ($\vec{B}=\vec{B}_0$) and accounting the shear field $\vec{B}_{0y}=\hat{y}B_0\tanh(x/L)$ along the $\hat{y}$ direction, Equation (12) can be written as

$$\frac{\partial\tilde{\psi}}{\partial t}+c\left(\frac{\partial}{\partial z}+\frac{B_{0y}}{B_0}\frac{\partial}{\partial y}+\frac{b_x}{B_0}\frac{\partial}{\partial x}+\frac{b_y}{B_0}\frac{\partial}{\partial y}\right)\phi-c\rho_s^2\nabla_\perp^2\left(\frac{\partial}{\partial z}+\frac{B_{0y}}{B_0}\frac{\partial}{\partial y}+\frac{b_x}{B_0}\frac{\partial}{\partial x}+\frac{b_y}{B_0}\frac{\partial}{\partial y}\right)\phi-\frac{c^2m_e\nabla_\perp^2}{4\pi n_0e}\frac{\partial\tilde{\psi}}{\partial t}=0. \quad (13)$$

Equation (13) can be written as (using $b_x=\frac{\partial\tilde{\psi}}{\partial y}$, $b_y=-\frac{\partial\tilde{\psi}}{\partial x}$)

$$\frac{\partial\tilde{\psi}}{\partial t}+c\left(\frac{\partial}{\partial z}+\frac{B_{0y}}{B_0}\frac{\partial}{\partial y}+\frac{1}{B_0}\frac{\partial^2\tilde{\psi}}{\partial x\partial y}-\frac{1}{B_0}\frac{\partial^2\tilde{\psi}}{\partial x\partial y}\right)\phi-c\rho_s^2\nabla_\perp^2\left(\frac{\partial}{\partial z}+\frac{B_{0y}}{B_0}\frac{\partial}{\partial y}+\frac{1}{B_0}\frac{\partial^2\tilde{\psi}}{\partial x\partial y}-\frac{1}{B_0}\frac{\partial^2\tilde{\psi}}{\partial x\partial y}\right)\phi-\frac{c^2m_e\nabla_\perp^2}{4\pi n_0e}\frac{\partial\tilde{\psi}}{\partial t}=0. \quad (14)$$

Equation (14) can be re-written as

$$\frac{\partial\tilde{\psi}}{\partial t}+c\left(\frac{\partial}{\partial z}+\frac{B_{0y}}{B_0}\frac{\partial}{\partial y}\right)\phi-c\rho_s^2\nabla_\perp^2\left(\frac{\partial}{\partial z}+\frac{B_{0y}}{B_0}\frac{\partial}{\partial y}\right)\phi-\frac{c^2m_e\nabla_\perp^2}{4\pi n_0e}\frac{\partial\tilde{\psi}}{\partial t}=0. \quad (15)$$

The scalar potential and vector potential are related as (using Equations (4) and (7) in (6))

$$\frac{\partial\left(\nabla_\perp^2\phi\right)}{\partial t}=\frac{v_A^2}{c}\left(\frac{\partial}{\partial z}+\frac{B_{0y}}{B_0}\frac{\partial}{\partial y}+\frac{b_x}{B_0}\frac{\partial}{\partial x}\right)\left(\nabla_\perp^2\tilde{\psi}\right). \quad (16)$$

Equations (15) and (16) are similar to Equations (6.77) and (6.78) of Biskamp (2000) with $\eta=0$ and $\mu=0$ by substituting $n=d_iw_i/B$ from Equation (6.79). One can get linear growth rate of tearing instability using Equations (6.92) and (6.93) which are derived using Equations (6.77) and (6.78) in Biskamp (2000). But our main purpose here is to study the dynamical evolution of the magnetic island. Therefore, we proceed as follows: Now if consider linear case, we get the relation between the scalar potential and vector potential as given below:

$$\frac{\partial\phi}{\partial t}\approx\frac{v_A^2}{c}\left(\frac{\partial}{\partial z}+\frac{B_{0y}}{B_0}\frac{\partial}{\partial y}\right)\tilde{\psi}. \quad (17)$$

Eliminating $\phi$ in Equation (15) by using Equation (17), we get

$$\frac{\partial^2\tilde{\psi}}{\partial t^2}-\lambda_e^2\frac{\partial^2}{\partial x^2}\frac{\partial^2\tilde{\psi}}{\partial t^2}-v_A^2\left(1-\rho_s^2\frac{\partial^2}{\partial x^2}\right)\left(\frac{\partial^2}{\partial z^2}+\frac{B_{0y}^2}{B_0^2}\frac{\partial^2}{\partial y^2}+\frac{2B_{0y}}{B_0}\frac{\partial^2}{\partial y\partial z}\right)\tilde{\psi}=0. \quad (18)$$

Here,

$$\lambda_e=\left(m_ec^2/4\pi n_0e^2\right)^{1/2}$$

is the electron inertial length, $\rho_s=c_s/\omega_{ci}$is ion gyroradius and$c_s=(k_BT_e/m_i)^{1/2}$ is the ion sound velocity. After the normalization, Equation (18) can be written as

$$\frac{\partial^2\tilde{\psi}}{\partial t^2}-c_1\frac{\partial^2}{\partial x^2}\frac{\partial^2\tilde{\psi}}{\partial t^2}-\left(1-\frac{\partial^2}{\partial x^2}\right)\left(\frac{\partial^2}{\partial z^2}+(\tanh(0.2x))^2\frac{\partial^2}{\partial y^2}+2\tanh(0.2x)\frac{\partial^2}{\partial y\partial z}\right)\tilde{\psi}=0. \quad (19)$$

Here $c_1=\lambda_e^2/\rho_s^2$. The normalization constants are

$$x_n=\rho_s,\ \ y_n=1/k_y,\ t_n=1/k_yv_A$$

and the normalized profile for Harris equilibrium field $B_{0y}/B_0=\tanh(0.2x)$ (Harris 1962).

Next, to investigate the effect of background field on the evolution of magnetic islands, we have divided our study in two different cases. In Case I, we ignore the axial magnetic field and consider only the Harris equilibrium field. Whereas, in Case II, we take both the fields which is a more generalized case when studying the magnetopause reconnection as magnetic fields involved in magnetopause reconnection are from different origins but can still have a parallel field component or axial background field.

*Case I.* If axial field is neglected, then Equation (19) can be written as

$$\frac{\partial^2\tilde{\psi}}{\partial t^2}-c_1\frac{\partial^2}{\partial x^2}\frac{\partial^2\tilde{\psi}}{\partial t^2}-\left(1-\frac{\partial^2}{\partial x^2}\right)\left((\tanh(0.2x))^2\frac{\partial^2}{\partial y^2}\right)\tilde{\psi}=0. \quad (20)$$

In order to get the dynamical equation we used the solution i.e., island profile, since magnetic reconnection is visualized within the framework of magnetic islands, as mentioned by Fitzpatrick and Waelbroeck (2005), i.e., $\tilde{\psi} = \psi_0''(-x^2/2 + b_0(x,t)\cos(y))$ in Equation (20). It can be written as ($b_0$ is the width of the magnetic island)

$$\frac{\partial^2 b_0}{\partial t^2} - c_1 \frac{\partial^4 b_0}{\partial x^2 \partial t^2} + \left(1 - \frac{\partial^2}{\partial x^2}\right)((\tanh(0.2x))^2) b_0 = 0. \tag{21}$$

*Case II.* Using the solution of vector potential

$$\tilde{\psi} = \psi_0''(-x^2/2 + b_0(x,t)\cos(y+z))$$

in Equation (19), we get the following equation:

$$\left(1 - c_1 \frac{\partial^2}{\partial x^2}\right) \frac{\partial^2 b_0}{\partial t^2} + \left(1 - \frac{\partial^2}{\partial x^2}\right) (1 + \tanh(0.2x))^2 b_0 = 0. \tag{22}$$

For simulation purpose, taking the magnetopause parameters (Chaston *et al.* 2008) $B_0 = 31 \times 10^{-5}$ G, $T_e = 37$ eV, $n_0 = 21\,\mathrm{cm}^{-3}$. Using these values, one finds that $\omega_{ci} = 3.1\,\mathrm{rad\,s}^{-1}$, $\omega_{pe} = 2.5 \times 10^5\,\mathrm{rad\,s}^{-1}$, $\lambda_e = 1.2 \times 10^5$ cm, $v_A = 1.1 \times 10^7\,\mathrm{cm\,s}^{-1}$, $\rho_s \approx 2.0 \times 10^6$ cm, $k_y = k_z = 1.0 \times 10^{-7}\,\mathrm{cm}^{-1}$, and the normalizing parameters are $c_1 = 0.05 x_n = 2 \times 10^6$ cm, $y_n = 1 \times 10^7$ and $t_n = 1.10$ s.

## 3. Numerical simulation and results

To solve the resulting dynamical equations numerically, we have used the finite difference method including a predictor corrector scheme for temporal evolution with time step $\Delta t = 10^{-5}$ and pseudo spectral method for space integration. Before embarking on the numerical solution of our present set of equations, we have tested the accuracy of our numerical code by monitoring the conservation of plasmon number viz. $N = \sum_k |\psi_{zk}|^2$ for the well-known nonlinear Schrödinger equation. We found that the plasmon number remains constant up to the sixth decimal place showing an accuracy of $10^{-6}$ throughout our computation. The code was then modified for solving the present dynamical equations (21) and (22) for both the cases I and II, respectively as described in the Section 2. Numerical simulation of Equations (21) and (22) is performed by using the constant initial condition for the initial width parameter $b_0(x,t) = 5$, having a size $2\pi/\alpha$ with 128 grid points (here$\alpha$ is the normalized perturbation wave number).

Figure 1(a)–(d) display the contour plot of vector potential in $x$–$y$ plane due to the sole presence of Harris field (absence of axial field) at different times, viz. (a) $t = 0$, (b) $t = 1$, (c) $t = 15$ and (d) $t = 45$. Here we can see that initially, there was a chain of magnetic islands which gets elongated along the $x$-axis with the advancement of time. Also, there is distortion in structures at a later time. Figure 2(a)–(d) are the contour plots of vector potential ($\psi$) in the $x$–$y$ plane due to the simultaneous presence of axial field as well as Harris field at different times viz. (a) $t = 0$, (b) $t = 1$, (c) $t = 15$ and (d) $t = 45$. Here we can see that modified structures with high intensity are formed at the advancement in time. The resulting structures are the indication of turbulence generation and hence the resulting power spectrum (Fig. 3). From these obtained results, it can be concluded that when the axial field is taken into account, electron dynamics come into the picture. Localization of the field gives rise to coherent structures and the reconnection process becomes faster when both the fields are present which can be seen in these figures. In the present work, the term $((\tanh(0.2x))^2 b_0(x,t))$ gives the interaction in the modes just like in nonlinear case. This product term is responsible for the evolution of island width to be irregular in space and time and ultimately in generation of turbulence. Similar type of situation where magnetic field fluctuations are observed experimentally solely due to inhomogeneity, has been reported by Scime *et al.* (2007) and numerical simulation (Goyal *et al.* 2015) work has also been analysed. Moreover, Finn and Kaw (1977) have also discussed closeness of islands due to inhomogeneity only. Therefore, the turbulence generation in the present work is solely due to inhomogeneity in the magnetic field (Harris field).

In Fig. 3, we have presented the power spectrum (spectral index $k^{-3/2}$ line is for only the reference and not the fit) for the second case when both axial field and Harris field are present. Chaston *et al.* (2008) have presented the power spectrum using the THEMIS data for the magnetopause region. Daughton *et al.* (2011) have done numerical simulation to discuss the turbulence generation in magnetopause plasma. Therefore, the present power spectrum has also demonstrated the signature of turbulence in the magnetopause reconnection site.

This steepening in the power spectrum will lead to the formation of thermal tail as a result of turbulence,

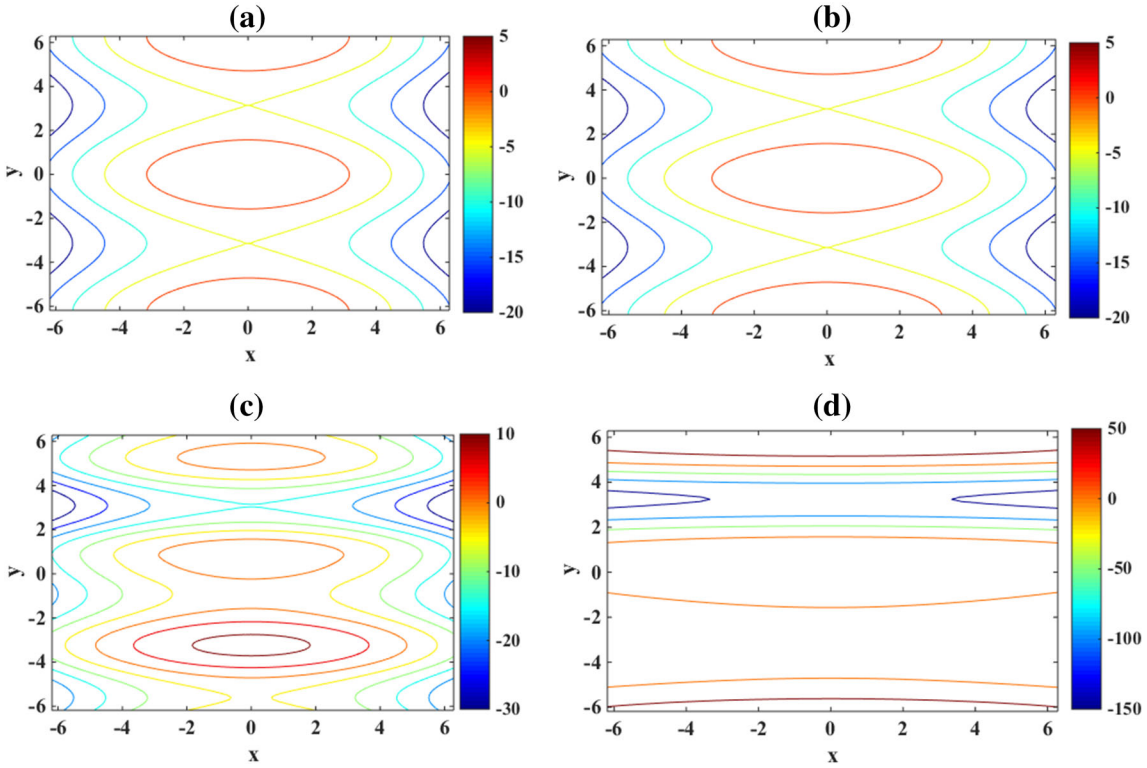


**Figure 1.** (**a**)–(**d**) The contour plot of vector potential ($\psi$) in the $x$–$y$ plane due to the sole presence of Harris equilibrium field (absence of axial field) at different times viz. (**a**) $t = 0$, (**b**) $t = 1$, (**c**) $t = 15$ and (**d**) $t = 45$.

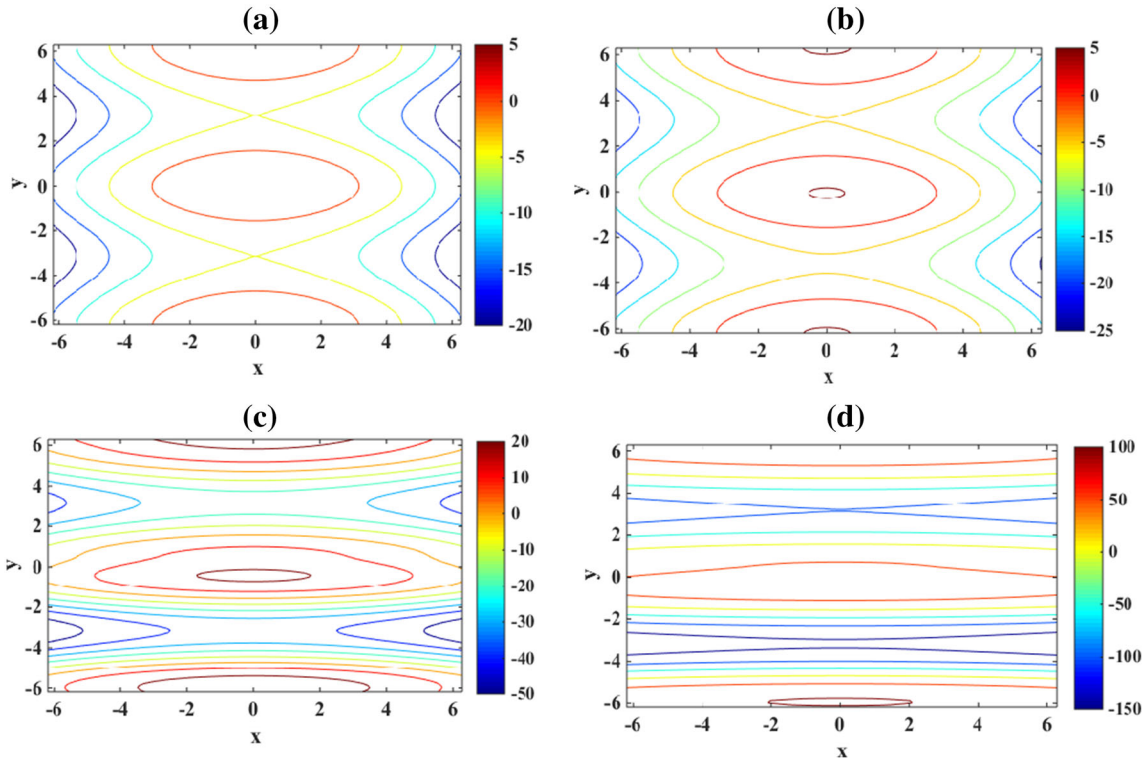


**Figure 2.** (**a**)–(**d**) The contour plot of vector potential ($\psi$) in the $x$–$y$ plane due to the simultaneous presence of axial field as well as Harris field at different times viz. (**a**) $t = 0$, (**b**) $t = 1$, (**c**) $t = 15$ and (**d**) $t = 45$.

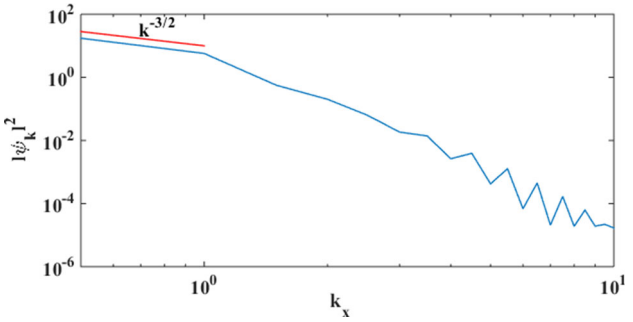


**Figure 3.** Turbulent spectrum resulting due to the simultaneous present of axial field and Harris equilibrium field.

which is believed to be responsible for the particle acceleration. Many authors have discussed the possible role of compressional turbulence in the particle acceleration. Sharma *et al*. (2016) have proposed that steepening in the power spectrum may lead to the thermal tail having a spectral shape $g(v) \propto v^{-4}$. They have used fractional diffusion approach to explain the thermal tail, which may be responsible for particle acceleration. In this approach, at the given time distribution function, $[g(v,t)]$ is expressed as $g(v) \sim v^{-(1+\mu)}$, where $\mu$is spectral index (Bian & Browning 2008). Similarly, in the present work, by taking the value of spectral index $\mu \approx 3/2$, we get the distribution function $g(v) \sim v^{-5/2}$. Hence it will lead to the enhancement of the thermal tail of the energetic electrons, which is responsible for the particle acceleration.

## 4. Summary and conclusion

This paper highlights on the evolution of the magnetic islands as a consequence of the Harris equilibrium field with and without the axial field. For this purpose, we have derived the dynamical equation to study the evolution of islands in the presence of background field comprising of both axial and Harris equilibrium field. Numerical simulation is performed to study the effect of electron dynamics in the evolution of magnetic islands. Simulation results reveal electron dynamics are important in the formation of current sheet and give signatures about the turbulent behavior of the system. Further, we have also evaluated the turbulent power spectrum which shows the distribution of power in wavenumber domain. The turbulence in power spectrum may lead to enrichment of the thermal tail of the energetic particles.

## Acknowledgements

This work is supported by Indian Space Research Organization (ISRO) (Grant No. ISRO/RES/2/415/17-18), India RESPOND Project.

## References

Ambrosiano J., Matthaeus W. H., Goldstein M. L., Plante D. 1988, J. Geophys. Res. Space Phys., 93(A12), 14383, https://doi.org/10.1029/JA093iA12p14383
Bhattacharjee A., Huang Y. M., Yang H., Rogers B. 2009, Phys. Plasma, 16, 112102
Bian N. H., Browning P. K. 2008, Astrophys. J. Lett. 687, L111
Biskamp D. 2000, Magnetic Reconnection in Plasmas. Cambridge Univ. Press, Cambridge
Burch J. L. *et al*. 2016, Science, 352(6290), aaf2939
Chaston C. C. *et al*. 2008, Nat. Phys., 4, 19
Chen L.-J. *et al*. 2008, Nat. Phys., 4, 19
Daughton W., Scudder J., Karimabadi H. 2006, Phys. Plasmas, 13, 072101
Daughton W., Roytershteyn V., Karimabadi H., Yin L., Albright B. J., Bergen B., Bowers K. J. 2011, Nat. Phys., 7, 539
Dong Q. L., Wang S. J., Lu Q. M., Haung C., Yuan D.-W., Liu X., Lim X., Li Y. T., Wei H.-G. *et al*. 2012, Phys. Rev. Lett., 108, 215001
Eastwood J. P., Phan T. D., Bale S. D., Tjulin A. 2009, Phys. Rev. Lett., 102, 035001
Finn J. M., Kaw P. K. 1977, Phys. Fluids, 20, 72
Fitzpatrick R., Waelbroeck F. L. 2005, Phys. Plasma., 12, 022308
Fu X. R., Lu Q. M., Wang S. 2006, Phys. Plasma, 13, 012309
Goyal R., Sharma R. P., Scime E. E. 2015, Phys. Plasma, 22, 022101
Harris E. G. 1962, Il Nuovo Cimento, XXIII, 115
Matthaeus W. H., Lamkin S. L. 1985, Phys. Fluids, 28, 303
Parker E. N. 1957, J. Geophys. Res., 62, 509
Parker E. N. 1979, Cosmical Magnetic Fields: Their Origin and Activity, Clarendon Press, Oxford
Scime E., Hardin R., Biloiu C., Keesee A. M., Sun X. 2007, Phys. Plasmas, 14, 043505
Sharma P., Yadav N., Sharma R. P. 2016, Solar Phys., 291, 931
Sweet P. A. 1958, Electromagnetic Phenomena in Cosmical Physics, IAU Symposium 6, 123
Takasao S., Asai A., Isobe H., Shibata K. 2016, Astrophys. J., 828, 103
Wang R. S., Lu Q. M., Du A. M., Wang S. 2010, Phys. Rev. Lett., 104, 175003